

doi:10.15199/48.2016.11.37

Effect of Uncertain Reference Signal on Uncertainty of estimates of the First Order PMD in a Single Mode Optical Fibre

Abstract. Joint probability density function of estimation errors of DGD and power split factor, the parameters defining the first order Polarization Mode Dispersion in an optical fibre, is formulated and used as a tool for investigation of influence of uncertainty of the reference signal, required by PMD measurement method, on uncertainty of the estimates. With the application of confidence intervals the uncertainty is evaluated through numerical analysis. Results can be applicable to PMD monitoring in optical fibre communications.

Streszczenie. Sformułowano model łącznego rozkładu prawdopodobieństwa błędów estymacji DGD i współczynnika podziału mocy, parametrów opisujących dyspersję polaryzacyjną I rzędu w światłowodzie, który użyto jako narzędzia do zbadania wpływu niepewności sygnału referencyjnego, wymaganego przez metodę pomiaru PMD, na niepewność estymat. Z zastosowaniem przedziałów ufności niepewność estymat została oceniona metodą analizy numerycznej. Rezultaty mogą znaleźć zastosowanie w monitorowaniu PMD w komunikacji światłowodowej. (Wpływ niepewności sygnału referencyjnego na niepewność estymacji parametrów PMD I rzędu w światłowodzie jednomodowym).

Keywords: polarization mode dispersion, dispersion monitoring, parameter estimation, estimator uncertainty.

Słowa kluczowe: dyspersja polaryzacyjna, monitorowanie dyspersji, estymacja parametrów, niepewność estymatora.

Introduction

Polarization mode dispersion (PMD) effects cannot be neglected in an on-off-keying (OOK) fibre optic direct detection communication line if transmission data rate is in the range of 10 Gbps or higher. Due to the PMD phenomenon waveforms of a transmitted signal can be distorted to an extent at which transmitted symbols cannot be retrieved with satisfactory low probability of error. A solution to PMD related limitations to optical communications can be an active management of fibers or wave-paths that is based on continuous in-work monitoring of at least the first order PMD in optical paths [1]. One particular method for monitoring PMD is based on learning parameters that describe the first order PMD, the differential group delay (DGD) and the power split factor between polarization modes, from distortions of the received waveform resulting from PMD. In this method a reference signal, free from PMD effect, is necessary [2]. The estimates of PMD parameters are obtained on the basis of the inverse problem principle with the use of an adequate model of PMD in an optical fibre [3]. For such a PMD monitoring system uncertainty of estimates of the first order PMD parameters was investigated under limiting assumption of negligible reference signal uncertainty [4]. The insight into the more general case is still lacking. In [2] it was shown that in a typical optical communications application scenario the maximum likelihood (ML) solution to the inverse problem, that effects the estimates, can be the minimum square error (MSE) estimation. If the postulate of negligible uncertainty of the reference signal cannot be fulfilled the MSE estimator may be no longer the ML one and moreover, it can suffer extra errors, in general of both static and random types. The aim of the paper is to learn to what level possible uncertainty of the reference signal can be tolerated while the use of the MSE estimation is extended to this more general case. Knowledge that allows to answer the above question can be instructive for engineering the monitoring system with the aim to provide satisfactory quality of the PMD measurements. Due to limited space here the focus of the analysis is on uncertainty of estimates, although general formulation provided allows to evaluate how biased the estimates are. Results of these evaluations will be published elsewhere.

The paper is organized as follows. It starts from brief description of a design and functioning of the system for in-work monitoring of the first order PMD (Section 1). Then the MSE type estimator of the first order PMD parameters is

introduced (Section 2). In the Section 3 an approximation is proposed that leads to an analytic model for joint probability density of estimation errors distribution. Then the model is compared against simulation data. In the Section 4 uncertainty of the estimates is assessed within targeted value range of the first order PMD parameters to be monitored. Conclusions summarize the results in the Section 5.

The system for in-work monitoring of the first order PMD in an optical fibre

In the system for in-work monitoring of the first order PMD, the measuring quality of which is addressed in this paper, intensity (power) samples of the transmitted waveforms are being taken at both ends of communications channel under monitoring. A separate data network is used to send the information on the signal being sampled at the input of the line to the receiving end (see the Fig. 1).

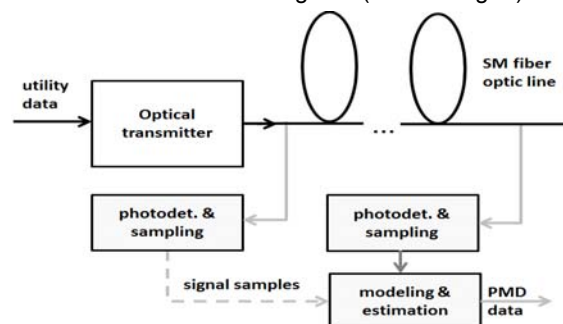


Fig. 1. The system for in-work monitoring of PMD parameters in a communications optical fibre line

In the simplest case this information can be the input signal samples themselves. In a more sophisticated variant however, the required information can be reduced to coefficients (parameters) of static and dynamic characteristics of the optical transmitter [5] being some way estimated from the input signal samples. Samples are being taken using synchronous undersampling principle, like in sampling oscilloscopes, hence sampled waveforms are virtually reproduced with substantially shorter effective sample spacing T_e than original sampling is done. It is assumed that synchronization allows an integer number of samples per bit. The signal samples collected at input and output are processed to effect MSE estimates of the PMD parameters with the use of a PMD model.

Mathematical description of the first order PMD parameter estimation

The phenomena governing propagation of a carrier in an optical fibre are well recognized. Optical waveforms undergo distortions due to linear effects: chromatic dispersion and polarization mode dispersion as well as nonlinear effects, among which the Kerr effect is typically the dominating mechanism and, due to interactions between linear and nonlinear phenomena. Except optical fibre also other optical components, like splitters, filters, multiplexers, which are used to build an optical fibre communications line, exhibit chromatic and polarization mode dispersion or spectral filtration. Optical amplifiers may be a source of extra distortions due to nonlinear phenomena including gain saturation, polarization hole burning, nonlinear dispersion as well as of optical noise, mainly of amplified spontaneous emission (ASE) type [6]. All this builds complex description on how optical carrier is being affected during propagation through an optical communications line. However, it is a typical practice in optical fibre communications engineering to have chromatic dispersion compensated in a distributed manner, along length of a communications line. This may cancel or substantially decrease the distortions due to chromatic dispersion and reduces accumulation of the distortions resulting from interaction between linear and nonlinear effects. Further, if only a few thoroughly spaced wavepaths are exploited in the optical fibre and the total optical power in the fibre remains below certain threshold the nonlinear effects can be neglected [6]. In [7] optical power thresholds are given which, when observed, allow not to exceed certain error levels in DGD estimation in the measurement system considered in this paper. In the following, only the simplest scenario is analysed in which an optical fibre line operates in a single channel regime, with chromatic dispersion effects cancelled through adequate compensation and, in which optical power is low enough to neglect influence of nonlinear phenomena.

The first order polarization dispersion manifests as propagation time difference (group delay) between two orthogonal polarization modes between which the total optical power of the propagating signal is split. Hence, two parameters are sufficient to describe the effect: the differential group delay (DGD) and the power split factor. The received (output) optical signal corresponds to a mix of both polarization modes. Photodetection results:

$$(1) \quad y(t) = \gamma r\left(t - \frac{\tau}{2}\right) + (1 - \gamma)r\left(t + \frac{\tau}{2}\right)$$

where: $r(t)$ and $y(t)$ are electrical equivalents of optical power of the transmitted and the output optical signals respectively, while τ is the DGD and γ is the power split factor. The formula (1) can be used to relate vectors of samples of $r(t)$ and $y(t)$ after time continuous functions are replaced with corresponding vectors. Please note however, that while the signals are represented now by vectors of discrete time samples, the domain of time delays by $\pm 0.5\tau$ in (1) is continuous. Then, obtaining samples of a delayed signal requires interpolation. In practice, $r(t)$ and $y(t)$ can be regarded bandlimited. Hence, Shannon-Whitaker formula may have an application here. With this stipulation in mind the vector version of the model (1) for PMD induced distortions to a signal being propagated in a fibre can be expressed as:

$$(2) \quad \mathbf{y} = \mathbf{m}(\mathbf{r}, \tau, \gamma)$$

where: \mathbf{r} and \mathbf{y} are vectors of collected samples of $r(t)$ and $y(t)$ respectively and each component of \mathbf{y} is computed from \mathbf{r} using (1) and interpolation according to which each y_k element of \mathbf{y} is given by:

$$(3) \quad y_k = \sum_{n=-0.5N}^{0.5N} d_n(\tau, \gamma) r_{k \oplus n}$$

with:

$$(4) \quad d_n(\tau, \gamma) = \gamma Sa\left(\pi\left(\frac{-\tau}{2T_e} - n\right)\right) + (1 - \gamma)Sa\left(\pi\left(\frac{\tau}{2T_e} - n\right)\right)$$

where: N is the number of signal samples, hence vector lengths, T_e is the effective sampling time interval, $Sa(x)$ is the sample function as used in the Shannon-Whitaker interpolation formula, \oplus operator denotes circular modulo N summation. Linear dependence between \mathbf{y} and \mathbf{r} , as dictated by (1), shall be minded in the following.

In the context of the monitoring system under consideration the \mathbf{y} vector in (2) represents output measurement data while the \mathbf{r} vector represents the reference signal (ref Fig. 2). Here both \mathbf{r} and \mathbf{y} are acquired with some uncertainty due to two statistically independent measurement noises. The random components of the \mathbf{r} and \mathbf{y} vectors will be denoted respectively by ζ and ξ . Statistical properties of ζ and ξ , given by corresponding joint density probabilities $\rho_\zeta(\zeta)$ and $\rho_\xi(\xi)$, are assumed known. It shall be noted that ξ and ζ are vectors of independent components which feature results from the use of synchronous undersampling principle that substantially spaces the samples in the time domain, believed to be beyond the range of non-negligible correlation. The MSE estimator effects the estimates minimizing the Euclidean distance between \mathbf{y} and $\mathbf{m}(\mathbf{r}, \tau, \gamma)$ vectors:

$$(5) \quad [\hat{\tau}, \hat{\gamma}]^T = f(\mathbf{r}, \mathbf{y}) = \underset{\tau \geq 0, 1 \geq \gamma \geq 0}{\operatorname{argmin}} \|\mathbf{y} - \mathbf{m}(\mathbf{r}, \tau, \gamma)\|$$

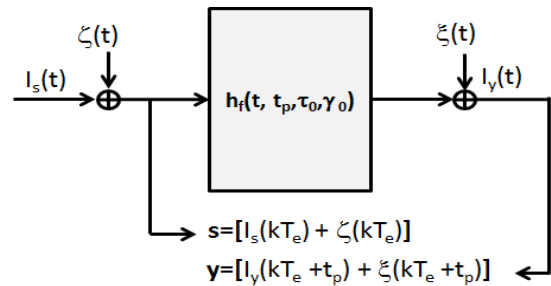


Fig. 2. The block diagram of the signal acquisition part of the first order PMD monitoring system

Modelling uncertainty of the MSE first order PMD estimates due to uncertain reference signal

Although the complete knowledge on estimate uncertainty can be learned from the joint probability distribution function (pdf) of the estimates of τ and γ this description can be too detailed, hence inconvenient for many practical applications. Usually, enough descriptive can be a confidence region that determines the minimum volume space (i.e. highest probability density space, HPD) of estimate values within which the estimates may fall with some prescribed confidence probability. Often a suitable parametrization of confidence regions is used to simplify description. Characterization of the first order PMD parameters requires two dimensional confidence regions.

In case of a general, non-Gaussian, pdf one can use confidence intervals (CI) which determine the minimum volume rectangular area that contains the 2D confidence region. Widths of the rectangular area edges may have meaning of widths of corresponding CIs (ref. Fig. 3 right panel). Such simplistic characterization provides no correlation information. However, it may be an option if either the correlation is of little use or, it is too complex to be

parametrized in a useful manner. In the paper widths of confidence intervals have been selected to characterize uncertainty of PMD estimates. Such a choice is motivated by results of the previous studies on uncertainty of estimates resulting from MLE estimation in the considered PMD monitoring system. It was revealed that, for the case when uncertainty of the reference signal is negligible, the joint pdf of estimation errors of the two first order PMD parameters can be highly non-Gaussian, particularly while DGD in a fibre under monitoring is low.

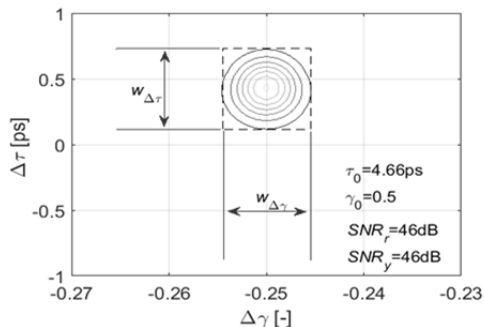


Fig. 3. Widths of confidence intervals for exemplary estimation error distributions of the first order PMD parameters

In order the assessment of estimate uncertainty could find a use in a design of the PMD monitoring system of interest the valuations need to be given under assumption that all constitutive quantities, necessary to calculate appropriate measures of estimation errors, like the actual PMD in a fibre or parameters of measurement noises, including noise variance etc., are known. This way objective measures of estimation error are obtained, as if the measurements were performed in a laboratory environment. This is the approach taken in the paper. Under this concept all error measure constitutive factors can be identified, recognized as either design dependent or independent, their influence quantified, hence directions for engineering of the monitoring system can be formulated with the intent to effect adequate measurement quality for a given application context.

For uncertainty characterization the underlying pdf of the estimates' errors, conditioned on known actual values of measurands, is the key. In case of the MSE estimator the start formula for the derivation of the joint pdf of estimation errors of the first order PMD parameters results from the necessary condition for a minimum of the square error between the output signal vector and the model (2) fed by the reference signal vector. The formula reads:

$$(6) \begin{cases} [\mathbf{m}(\boldsymbol{\chi}, \tau_0, \gamma_0) + \boldsymbol{\xi} - \mathbf{m}(\boldsymbol{\chi} + \boldsymbol{\zeta}, \tau, \gamma)]^T \frac{\partial \mathbf{m}(\boldsymbol{\chi} + \boldsymbol{\zeta}, \tau, \gamma)}{\partial \tau} = 0 \\ [\mathbf{m}(\boldsymbol{\chi}, \tau_0, \gamma_0) + \boldsymbol{\xi} - \mathbf{m}(\boldsymbol{\chi} + \boldsymbol{\zeta}, \tau, \gamma)]^T \frac{\partial \mathbf{m}(\boldsymbol{\chi} + \boldsymbol{\zeta}, \tau, \gamma)}{\partial \gamma} = 0 \\ \Delta \tau = \tau - \tau_0 \\ \Delta \gamma = \gamma - \gamma_0 \end{cases}$$

where: $\boldsymbol{\chi}$ is the vector of noiseless samples of the signal output by optical communications line transmitter, $\mathbf{y} = \mathbf{m}(\boldsymbol{\chi}, \tau_0, \gamma_0) + \boldsymbol{\xi}$, $\mathbf{r} = \boldsymbol{\chi} + \boldsymbol{\zeta}$, τ and γ are the estimates of the DGD and power split factor respectively, τ_0 and γ_0 denote actual values of these first order PMD parameters in the monitored fibre, $\Delta \tau$ and $\Delta \gamma$ are deviations of τ and γ from actual values of the corresponding measurands, i.e. are the estimation errors.

Previous studies [4] shown that $\mathbf{m}(\boldsymbol{\chi}, \tau, \gamma)$ cannot be linearized with respect to τ without loss of essential correlation information between the two estimates in the

joint pdf. Consequently, there is no an analytic solution for (6) and the pdf of interest can be approached only via approximations or computer simulations. In [4] an approximation was proposed that proved to follow considerably closely results of computer simulations for the case of negligible uncertainty of the reference signal. Unfortunately, the direct extension of this idea to the case considered in the paper, via adding reference signal measurement noise and proceeding with the same simplifications, does not work. It cannot explain well the biasing of the estimates that emerges with uncertainty of the reference signal, the effect shown in simulations (see Fig. 4).

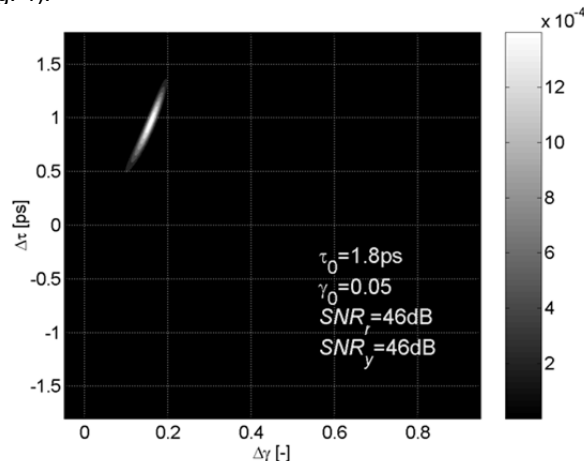


Fig. 4. Contour plots of estimation error 2D histograms obtained via simulations

A closer look at (6) reveals that in the two upper equations, except random terms (X_1 and X_2 respectively) that are linearly related to $\boldsymbol{\zeta}$ and $\boldsymbol{\xi}$ elements (measurement noise samples), there are non-negligible another random components (Y_1 and Y_2) which are sums of weighted squares of the $\boldsymbol{\zeta}$ noise vector elements with the weights dependent on τ and γ . In fact, Y_1 and Y_2 are responsible for the biasing effect. In case of large number of samples, (here $N > 500$), Y_1 and Y_2 can be considered Gaussian distributed tightly around their means which are proportional respectively to $N\sigma_\zeta^2$ and $N\sigma_\xi^2$ with individual scaling weights. Simulations shown that spreads of Y_1 and Y_2 are orders of magnitude smaller than spreads of X_1 and X_2 . Such an observation allows to approximate Y_1 and Y_2 only by their means. In consequence the estimates appear to be related to the X_1 and X_2 random terms as follows:

$$(7) \quad f_1(\tau, \gamma) = X_1 \quad f_2(\tau, \gamma) = X_2$$

where:

(8)

$$f_1(\tau, \gamma) = [\mathbf{m}(\boldsymbol{\chi}, \tau_0, \gamma_0) - \mathbf{m}(\boldsymbol{\chi}, \tau, \gamma)]^T \frac{\partial \mathbf{m}(\boldsymbol{\chi}, \tau, \gamma)}{\partial \tau} + g_1(\tau, \gamma) N \sigma_\zeta^2$$

$$f_2(\tau, \gamma) = [\mathbf{m}(\boldsymbol{\chi}, \tau_0, \gamma_0) - \mathbf{m}(\boldsymbol{\chi}, \tau, \gamma)]^T \frac{\partial \mathbf{m}(\boldsymbol{\chi}, \tau, \gamma)}{\partial \gamma} + g_2(\tau, \gamma) N \sigma_\zeta^2$$

$$(9) \quad X_1 = -[\boldsymbol{\xi} + \mathbf{m}(\boldsymbol{\zeta}, \tau_0, \gamma_0)]^T \frac{\partial \mathbf{m}(\boldsymbol{\chi}, \tau, \gamma)}{\partial \tau} \Big|_{\tau_0, \gamma_0}$$

$$X_2 = -[\boldsymbol{\xi} + \mathbf{m}(\boldsymbol{\zeta}, \tau_0, \gamma_0)]^T \frac{\partial \mathbf{m}(\boldsymbol{\chi}, \tau, \gamma)}{\partial \gamma} \Big|_{\tau_0, \gamma_0}$$

The two functions in (8) that appear in the components responsible for the bias are given by:

$$(10) \quad g_1(\tau, \gamma) = \mathbf{d}(\tau, \gamma)^T \frac{\partial \mathbf{d}(\tau, \gamma)}{\partial \tau}$$

$$g_2(\tau, \gamma) = \mathbf{d}(\tau, \gamma)^T \frac{\partial \mathbf{d}(\tau, \gamma)}{\partial \gamma}$$

where: $\mathbf{d}(\tau, \gamma)$ is the vector collecting $d_k(\tau, \gamma)$ functions for $k \in \langle 1, N \rangle$.

In (9) the ξ -dependent components, respectively in X_1 and X_2 , are two jointly Gaussian distributed random variables with zero means and certain correlation matrix, say Σ_ξ . Analogous observation can be made for the pair of the ζ -dependent components of X_1 and X_2 . Their correlation matrix will be denoted by Σ_ζ . Elements of both matrices are given as follows:

$$(11) \quad s_{i,j} = 2\sigma^2 \sum_{n=1}^N V_{i,n} V_{j,n} \quad i, j = 1, 2$$

with:

$$(12) \quad V_{1,n} = \left[\frac{\partial \mathbf{m}(\chi, \tau, \gamma_0)}{\partial \tau} \Big|_{\tau_0} \right]_n \quad V_{2,n} = \left[\frac{\partial \mathbf{m}(\chi, \tau_0, \gamma)}{\partial \gamma} \Big|_{\gamma_0} \right]_n$$

and $\sigma = \sigma_\xi$ for Σ_ξ , and:

$$(13) \quad V_{1,n} = \sum_{k=1}^N d_{u(n,k)}(\tau_0, \gamma_0) \left[\frac{\partial \mathbf{m}(\chi, \tau, \gamma_0)}{\partial \tau} \Big|_{\tau_0} \right]_k$$

$$V_{2,n} = \sum_{k=1}^N d_{u(n,k)}(\tau_0, \gamma_0) \left[\frac{\partial \mathbf{m}(\chi, \tau_0, \gamma)}{\partial \gamma} \Big|_{\gamma_0} \right]_k$$

with $\sigma = \sigma_\zeta$ for Σ_ζ . The function $u(n,k)$ provides proper indices in summation. Both the ξ -dependent and the ζ -dependent pairs remain statistically independent. Then in conclusion, the X_1 and X_2 random variables are also jointly Gaussian distributed, have zero means and their correlation matrix $\Sigma = \Sigma_\xi + \Sigma_\zeta$. The above considerations lead to the following formulation for the joint pdf of estimation errors of the first order PMD parameters:

$$(14) \quad p(\Delta\tau, \Delta\gamma) = (2\pi)^{-1} |\Sigma|^{-0.5} \exp \left\{ -\frac{1}{2} \begin{bmatrix} f_1 \\ f_2 \end{bmatrix}^T \Sigma^{-1} \begin{bmatrix} f_1 \\ f_2 \end{bmatrix} \right\} \times$$

$$\times |J(f_1, f_2)| \times J(f_1, f_2) \times \left[J(f_1, f_2) \right]$$

in which $J(f_1, f_2)$ is Jacobian matrix and:

$$(15) \quad f_1 = f_1(\tau_0 + \Delta\tau, \gamma_0 + \Delta\gamma)$$

$$f_2 = f_2(\tau_0 + \Delta\tau, \gamma_0 + \Delta\gamma)$$

This is the same general formula as in [4] with $f_1(\tau, \gamma)$, $f_2(\tau, \gamma)$ and the covariance matrix Σ defined by new relations.

Before it was decided to use the model (14) for the intended characterization of uncertainty of the first order PMD estimates the model underwent verification. For this reason a number of simulations were run with the use of the VPI Transmission Maker simulation tool, a software system for photonics communication simulations. Within the targeted ranges of the first order PMD parameters, $\tau_0 \in \langle 1.5, 7.5 \rangle$ ps for the DGD and, $\gamma_0 \in \langle 0.05, 0.5 \rangle$ for the power split factor, a 20×20 matrix of equidistributed test points was created. Lower, than targeted, τ_0 and γ_0 values result in negligible distortions to an optical signal, hence estimation errors of the first order PMD lose practical importance when estimation results are used to evaluate transmission quality of an optical signal. The upper limit for the analysed DGD values satisfies typical needs of long distance optical fibre communications lines. In general, the power split factor can range between 0 and 1. However, physics of the PMD phenomena instructs that optical power

of PMD affected signal behaves symmetrically around $\gamma_0 = 0.5$.

For each test point the monitoring system, as shown in the Fig. 1, was simulated in 10^6 runs per point. Here, a PMD affected fibre was modelled by a PMD emulator, a part of VPI Transmission Maker library. The intended τ_0 and γ_0 values were parameters directly set in the emulator. The transmitter signal $\chi(t)$ was of 10 Gbps binary OOK type with $0.25T_b$ rise and fall times (T_b – bit slot time) driven by the pseudo-random PRBS7 sequence. Noise levels at sample acquisition points were adjusted through proper setting of dark currents in models of photodetectors. Following combinations of noise levels, given in terms of signal-to-noise ratios of $r(t)$ reference (SNR_r) and $y(t)$ output (SNR_y) signals, were used: $SNR_r = \{46, \infty\}$ dB and $SNR_y = \{40, 46, 52, 58\}$ dB. Per an estimate 1024 samples were acquired with effective 6.25 ps sampling period.

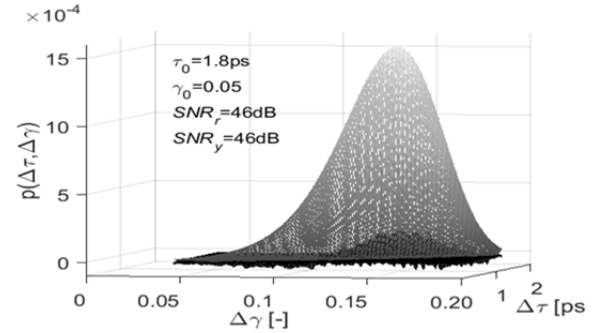


Fig. 5. Surface plot of the joint pdf of estimation errors computed from (16) and the difference between the model and the corresponding histogram (bottom black)

For each test point the monitoring system, as shown in the Fig. 1, was simulated in 10^6 runs per point. For each run the MSE joint estimator based on the formula (5) produced actual values of τ and γ . The recorded differences $\Delta\tau = \tau - \tau_0$ and $\Delta\gamma = \gamma - \gamma_0$ were used to build 500×500 2D estimation error histograms $h(\Delta\tau, \Delta\gamma, \tau_0, \gamma_0)$ for each test point. Every histogram was compared to the model (14) in the following way. For each $\Delta\tau$ value a 1-D histogram conditioned on $\Delta\tau$, $h(\Delta\gamma, \tau_0, \gamma_0 | \Delta\tau)$, was extracted and $\Delta\gamma$ average $\mu_{\Delta\gamma}(\tau_0, \gamma_0 | \Delta\tau)$, $\Delta\gamma$ standard deviation $\sigma_{\Delta\gamma}(\tau_0, \gamma_0 | \Delta\tau)$ and marginal value $p_m(\tau_0, \gamma_0 | \Delta\tau)$ were computed. In order to account for randomness of the above histogram there were obtained CIs at 0.99 level for every value of the mean, standard deviation and the marginal. Bootstrap method was used. The analysis confirmed that the model (14) with reasonable accuracy reproduces the shape of the underlying distribution of $\Delta\tau$ and $\Delta\gamma$ that have been obtained in simulations, in the entire tested range. The means and standard deviations from the model (14) agree well with those from simulations in regions of $\Delta\tau$ where frequencies of $\Delta\tau$ and $\Delta\gamma$ occurrence are non-negligible. To be more specific, within the HPD intervals of $\Delta\tau$ where the $\int p_m(\tau_0, \gamma_0 | \Delta\tau) d\Delta\tau \geq 0.99$, for the entire targeted τ_0 and γ_0 space and for all combinations of SNR_r and SNR_y , the maximum absolute differences between $\Delta\gamma$ means from (14) and corresponding CIs bounds from simulation were below 10^{-3} while between $\Delta\gamma$ standard deviations from (16) and corresponding CIs bounds were below $6 \cdot 10^{-2}$. Please refer the example illustrated in the Fig. 5 where the bottom black 2D part of the plot represents error between the model pdf and the histogram. The details are shown in the Fig. 6 where the $\Delta\gamma$ mean (left) and $\Delta\gamma$ standard deviation (right) conditioned on $\Delta\tau$, versus $\Delta\tau$ are depicted. For better clarity the plots show only the upper and lower (mid-grey dashed lines for both) CIs boundaries for either mean or standard

deviation. The black curve represents the corresponding parameter resulting from the model (14). The broken bright grey line shows behaviour of the marginal to indicate the region within which approximation error matters.

Uncertainty of the first order PMD parameters due to reference signal uncertainty

The following analysis exploits the model (14) of the first order PMD estimation errors joint distribution. Despite analytic formulation in (14) the relations between measures of uncertainties of the estimates of interest and uncertainty of the reference signal as well as actual first order PMD in a fibre under monitoring, remain complex. Hence, the only viable way for learning these relations is a numerical analysis. This forces to make assumptions regarding those parameters which are not of direct interest however, influence results. This concerns selection of a shape of the transmitted signal, transmitted data sequence, bit signaling interval length, sampling interval, optical and electrical filtering and, confidence level, to mention the most influential. Here, these questions were answered through making commonly agreed choices or a selection of a possibly enough representative example.

In the calculations the transmitted signal $\chi(t)$, data sequence, sampling, targeted range of DGD and power split factor were assumed as in the previous Section. No optical or electrical filtering was applied except that related to the PMD phenomenon. Transmitter signal samples were obtained from the VPI Transmission Maker simulation tool. Confidence level was assumed 0.95. A pdf value driven 2D integration algorithm yielded the confidence regions, boundaries of which provided CI widths. CIs were calculated on a 20×20 grid of τ_0 and γ_0 values, covering targeted τ_0 and γ_0 ranges, and for the following combinations of signal-to-noise ratios $SNR_y = \{46, \infty\}$ dB and $SNR_r = \{40, 46, 52, 58, \infty\}$ dB.

Numerical analysis reveals that, while level of uncertainty of the reference signal influences widths of CIs of the DGD and of the power split factor, the intensity of this effect depends on actual PMD (τ_0 and γ_0) in a fibre under monitoring. The widths maximize at the lower limits of the targeted measurement range of these quantities, irrespectively what SNR_r and SNR_y are. This general behaviour is illustrated in the Fig. 7 for an exemplary case where $SNR_r = 46$ dB and $SNR_y = \infty$. Generally, uncertainty of the reference signal adds to uncertainty of the τ and γ estimates with different scale than uncertainty of $y(t)$ does, provided equal SNRs. This effect is visible in the low DGD range while it gradually vanishes with DGD increase. For low actual DGD, at low SNR values, widths of CIs for τ estimate are more affected by uncertainty of $y(t)$ than that of $r(t)$. The lower is actual DGD the more emphasised is the difference. Analogous discrepancy is even more stressed for CIs of γ estimate. In particular, at low SNR_r the CI can even shrink with decrease of actual DGD, if estimate uncertainty solely results from $r(t)$ uncertainty, which is opposed to that case when it is caused by uncertainty of $y(t)$ only. Moreover, if the actual DGD is very low the CI of γ estimate can be narrower for low SNR_r when compared with that for higher SNR_r . In case of non-zero uncertainty of $y(t)$ the above behaviour is reproduced for γ estimate, and appears, for τ estimate, which is evidenced by bottom plots in the Fig. 8-9. Although the effect could seem anomalous, suggesting smaller estimation errors obtainable from more uncertain data, mind biasing of the estimates in low DGD range, particularly heavily at low SNR_r . Then, by no means more accurate estimation happens. The anomalous reduction of CI widths can be attributed to the shift of the joint pdf of estimation errors towards higher τ and γ values (observed at low SNR_r) at which the pdf shows smaller spread.

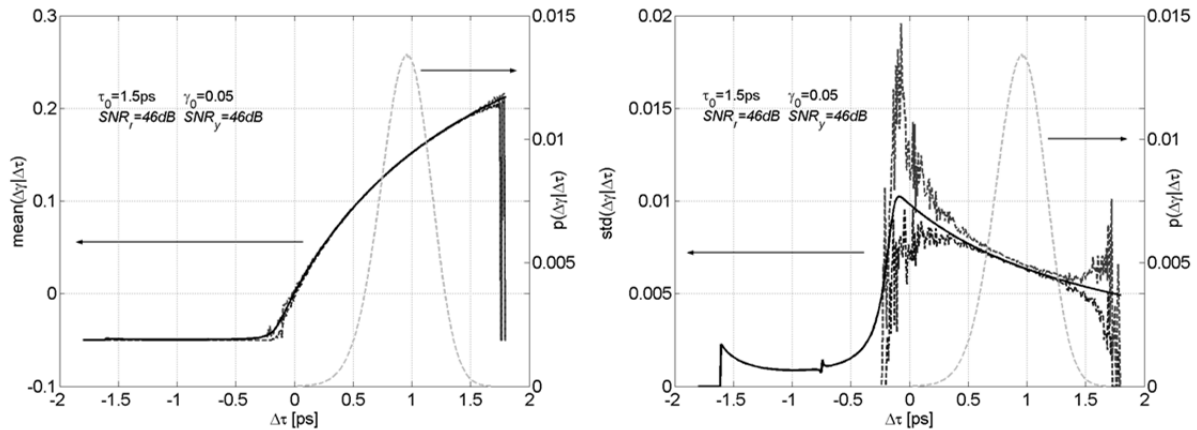


Fig. 6. Parametric comparison between pdf from model (14) and simulation data. Left - $\Delta\gamma$ means, right $\Delta\gamma$ standard deviations, both conditioned on $\Delta\tau$, versus $\Delta\tau$

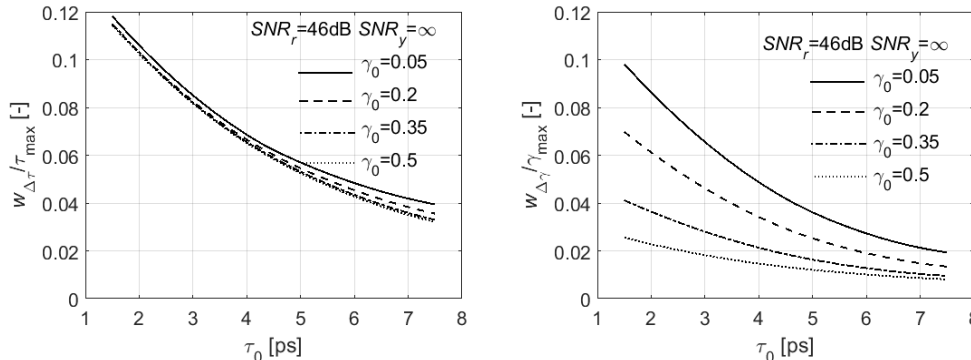


Fig. 7. Widths of confidence intervals for DGD estimates (left plot) and for power split factor estimates (right plot) versus actual DGD in a fibre. Actual power split factor is the parameter

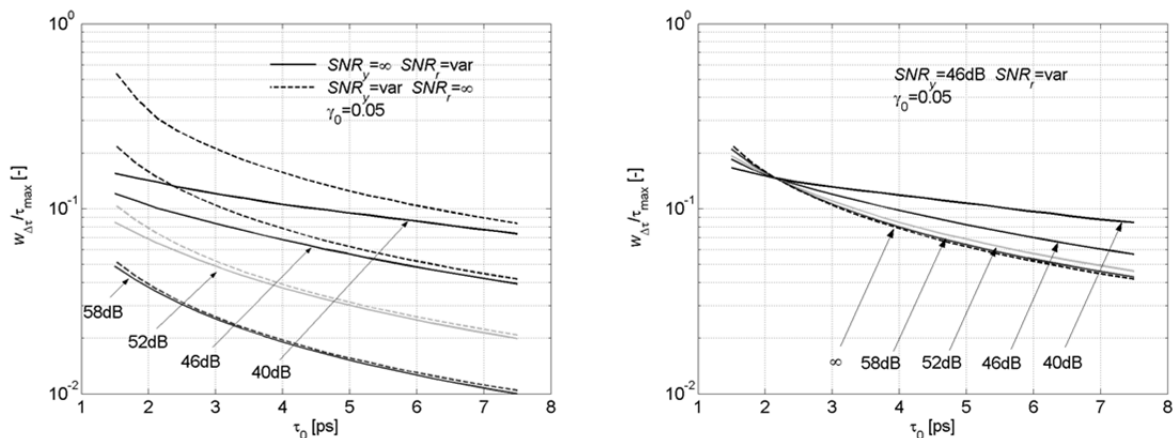


Fig. 8. Widths of confidence intervals for DGD estimates versus actual DGD in a fibre. SNR of the reference signal is the parameter

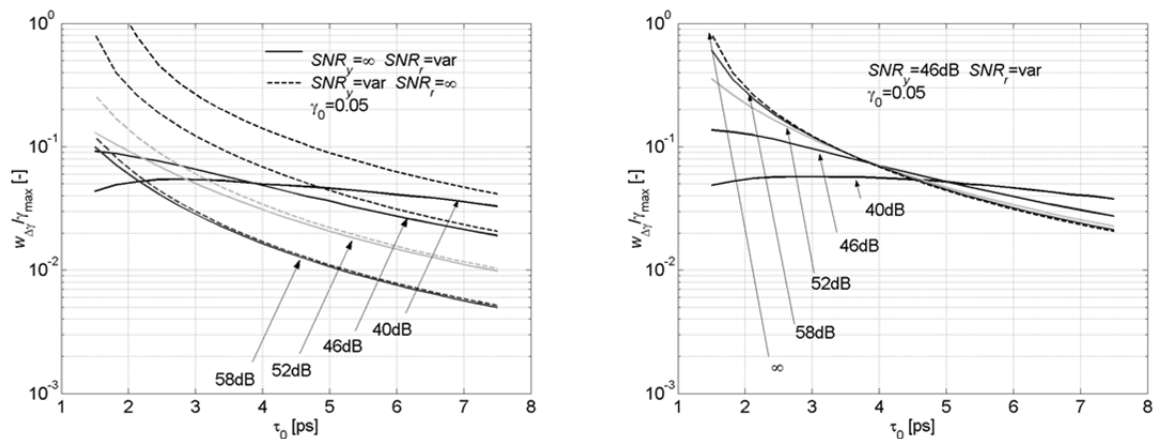


Fig. 9. Widths of confidence intervals for power split factor estimates versus actual DGD in a fibre. SNR of the reference signal is the parameter

In the Fig. 8-9 the top plots illustrate the hypothetical case where effects of uncertainty of $\gamma(t)$ are absent ($SNR_y = \infty$). Widths corresponding to this case are given by solid lines, for certain values of the SNR_r . For a comparison the widths resulting only from uncertainty of $\gamma(t)$ ($SNR_r = \infty$) for the same values of SNR are given by dash lines. The bottom plots correspond to a practical case where uncertainty of $\gamma(t)$ is non-zero. For a purpose of a design of the first order PMD monitoring system of interest the curves in the Fig. 8-10 instruct what uncertainty of both signals, that source data for PMD estimation, can be tolerated for a given targeted uncertainty of PMD estimates. The curves are shown only for the lowest extreme of the targeted γ_0 range because there the uncertainties maximize (ref. Fig. 7). On the both bottom plots the dash lines illustrate asymptotic behaviour corresponding to $SNR_r = \infty$.

Conclusions

In the first order PMD monitoring system the reference and output signals uncertainties cause errors of MSE estimates of PMD parameters, DGD and power split factor, that generally show non-Gaussian 2D distribution. Hence, the description of how uncertainty of the reference signal affects uncertainty of the estimates was made through widths of confidence intervals that bound a rectangular area containing the actual confidence area. The widths depend in a complex way on uncertainty of the reference signal and quantities defining PMD. One may focus on worst case analysis when an application is a design of the PMD monitoring system that satisfies a postulated level of measurement uncertainty. The worst case characteristics, provided in the paper, that quantify widths of confidence intervals for estimates of the two PMD parameters versus

uncertainties of acquired data and quantities defining PMD, can have direct application in such a design. In particular, required signal to noise ratios for the reference and output signals can be found. A general observation suggests that, in the considered monitoring system, uncertainty of the reference signal, expressed as SNR below 60dB is unlikely to provide estimates of measurands with sufficiently low uncertainty for a typical telecomm application.

Author: dr inż. Zbigniew Lach, Politechnika Lubelska, Instytut Elektroniki i Technik Informatycznych, ul. Nadbystrzycka 38a, 20-618 Lublin, E-mail: z.lach@pollub.pl

REFERENCES

- [1] Chan C.C., Optical Performance Monitoring. Advanced Techniques for Next-Generation Photonic Networks. Academic Press, Elsevier, Amsterdam, (2010), 67-92
- [2] Lach Z., Characterization of first order PMD measurements based on a transmitted signal in an OOK fiber optic communication line, *Proc. of SPIE*, 9228 (2014), 92280U
- [3] Tarantola A., Inverse Problem Theory and Methods for Model Parameter Estimation, SIAM, Philadelphia, (2005), 20-40
- [4] Lach Z., Tail of the joint distribution of the first order PMD parameters. *Proc. of SPIE*, 9816 (2015), 98160H
- [5] Lach Z., A method for identification of static and dynamic characteristics of a non-zero chirp Mach-Zehnder optical intensity modulator for application in OOK fiber optic communication line. *Elektronika: Konstrukcje, Technologie, Zastosowania*, 4, (2014), 28-31
- [6] Agrawal G. P., Nonlinear Fiber Optics, Academic Press, New York, (2001), 97-122
- [7] Lach Z., Limitations to inverse problem based estimation of DGD in an optical fiber due to the use of the linear propagation model. *Proc. of SPIE*, 9662 (2015), 966211